

Short Communication

## Microstructure and Corrosion Resistance of Ni-P/Ni-W-P/Ni-P Three-layer Coating Prepared on 45# Steel by Chemical Deposition Method

Bai Xue<sup>1,3,\*</sup>, Bai Rui<sup>1,2,3</sup>, Mu Miao<sup>1,2,3</sup>, Lu Cuiying<sup>1,3</sup>, Wang Jinxi<sup>1,2,3</sup>, Wang Aimin<sup>1,2,3</sup>

<sup>1</sup> School of Chemistry & Chemical Engineering, YuLin University, YuLin 719000, China;

<sup>2</sup> School of Chemical Engineering & Technology, China University of Mining and Technology, Xuzhou 221116, China;

<sup>3</sup> Shaanxi Key Laboratory of Low Metamorpcoal Clean Utilization, YuLin University, YuLin 719000, China;

\*E-mail: [Bai\\_edu719@163.com](mailto:Bai_edu719@163.com)

Received: 6 April 2022 / Accepted: 16 May 2022 / Published: 4 July 2022

---

Ni-P/Ni-W-P/Ni-P three-layer coating is prepared on 45# steel substrate by chemical deposition method. Meanwhile, the Ni-P coating with medium phosphorus content is as the bottom layer, Ni-W-P coating is as the intermediate layer and the Ni-P coating with high phosphorus content is as the outer layer. The surface morphology, composition, microstructure and corrosion resistance of three-layer coating are characterized by scanning electron microscope, energy dispersive spectrometer, X-ray diffraction and electrochemical workstation respectively. The results show that three-layer coating has an amorphous structure with a small amount of microcrystalline structure, its porosity is only 1.54% and the surface compactness is better than that of Ni-P single-layer coating. The main composition of three-layer coating is Ni, P and W elements, which belongs to the coating with high phosphorus content. The corrosion current density of three-layer coating without immersion is  $7.24 \times 10^{-7}$  A/cm<sup>2</sup>, which is nearly two orders of magnitude lower than that of 45# steel substrate. The corrosion rate of three-layer coating without immersion is only 0.044 g/(cm<sup>2</sup>·a), which is lower than that of 45# steel substrate. After immersion in 3.5% sodium chloride solution for 14 days, the corrosion degree of three-layer coating is very light, and the corrosion current density increases very slowly, indicating that the corrosion resistance of three-layer coating is better than that of single-layer coating, which can provide better protection for 45# steel substrate.

---

**Keywords:** Ni-P/Ni-W-P/Ni-P three-layer coating; Ni-P single-layer coating; Chemical deposition method; Microstructure; Corrosion resistance

## 1. INTRODUCTION

Nickel-based alloy coatings (including Ni-P coating, Ni-Co-P coating, Ni-W coating, etc.) have bright appearance and dense microstructure with good corrosion resistance, excellent wear resistance and great oxidation resistance which is suitable for used as decorative and functional coatings [1-4]. Electrodeposition method or chemical deposition method can be used to prepare nickel-based alloy coatings reported by many scholars [5-8]. Chemical deposition method does not require external power supply and anode, which can avoid the problem of inhomogeneous thickness of the coating caused by uneven current distribution. In addition, compared with electrodeposition method, chemical deposition method has the advantages of lower cost, convenient operation and better controllability, which is more suitable for preparing nickel-based alloy coatings [9-12].

However, the unit cell of the nickel-based single-layer coating is not tightly combined resulting in some holes on the surface with poor corrosion resistance which makes it difficult to meet the requirements of many applications. Some studies have shown that the multi-layer coating prepared by deposition method on the basis of single-layer coating showed excellent corrosion resistance and could make up for the performance defects of the single-layer coating [13-18]. At present, there are few reports on the preparation of nickel-based three-layer coating by chemical deposition method. It is necessary to continue to research in this area to provide more reference. In this paper, Ni-P/Ni-W-P/Ni-P three-layer coating was prepared on the surface of 45# steel by chemical deposition method, and its composition, microstructure and corrosion resistance were characterized and analyzed to compare with the Ni-P single-layer coating.

## 2. EXPERIMENTAL

### 2.1 Materials and chemical reagents

The substrate is 45# steel, which is cut into 40 mm × 20 mm × 1 mm size. The samples pretreatment process is as follows: (1) polished with 800#, 1200# and 2000# sandpaper in turn; (2) cleaned by ultrasound in acetone for 5 min; (3) deionized water cleaning; (4) immersion in alkali solution (sodium hydroxide 40 g/L + sodium carbonate 8 g/L) at 65°C for 8 min; (5) immerse in 10% hydrochloric acid for 1 min until uniform bubbles are attached to the surface of the samples; (6) washed with deionized water; (7) dried with cold air.

The chemical reagents used in the experiment include: nickel sulfate, sodium hypophosphite, sodium tungstate, sodium citrate, emulsifier, lactic acid, sodium hydroxide, sodium carbonate, ammonium sulfate, sodium chloride, surfactant, etc.

### 2.2 Preparation of Ni-P/Ni-W-P/Ni-P three-layer coating

Figure 1 shows the schematic diagram of preparing Ni-P/Ni-W-P/Ni-P three-layer coating on the surface of the 45# steel substrate by chemical deposition method. The brief description is as follows:

Step 1: prepare three kinds of plating solution, the main components are shown in Table 1.

Step 2: immerse the 45# steel sample in plating solution I, and deposit for 30 min at a constant temperature of 84°C to prepare a Ni-P coating with medium phosphorus content as the bottom layer. After cleaning, the 45# steel sample is immersed in plating solution II, and is deposited for 60 min at a constant temperature of 92°C to prepare a Ni-W-P coating as the intermediate layer. Finally, the 45# steel sample is immersed in plating solution III, and deposit for 30 min at a constant temperature of 84°C to prepare a Ni-P coating with high phosphorus content as the outer layer.

Step 3: After cleaning the 45# steel sample, put it in an oven, set it to heat treatment at 200°C for 1 h, and release the internal stress of the coating.

In addition, the 45# steel sample is immersed in the plating solution I, and is deposited for 120 min at a constant temperature of 84°C to prepare a Ni-P single-layer coating as a comparison.

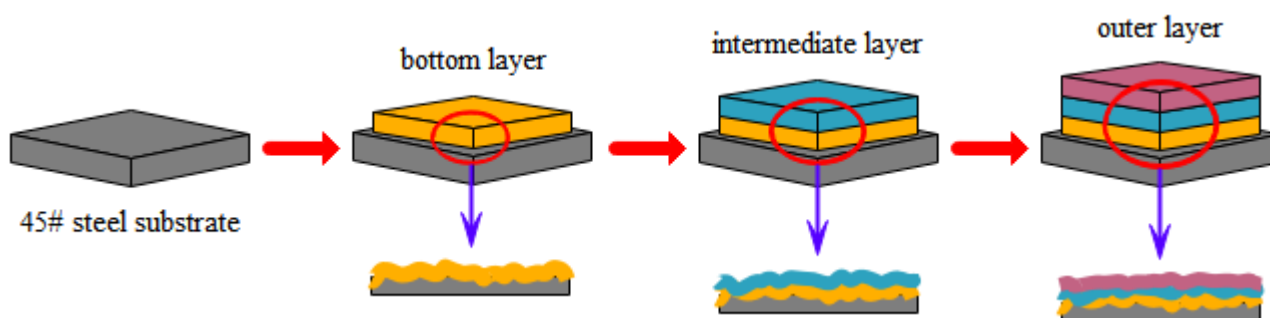


**Figure 1.** Schematic diagram of preparing Ni-P/Ni-W-P/Ni-P three-layer coating on the surface of 45# steel substrate by chemical deposition method

**Table 1.** Main components of different plating solutions

Chemical reagents	Plating solution I	Plating solution II	Plating solution III
$\text{Ni}_2\text{SO}_4/ (\text{g}\cdot\text{L}^{-1})$	24	20	26
$\text{NaH}_2\text{PO}_2/ (\text{g}\cdot\text{L}^{-1})$	28	40	32
$\text{C}_6\text{H}_5\text{Na}_3\text{O}_7/ (\text{g}\cdot\text{L}^{-1})$	10	30	20
$\text{Na}_2\text{WO}_4/ (\text{g}\cdot\text{L}^{-1})$	—	7.5	—
$\text{Na}_2\text{CO}_3/ (\text{g}\cdot\text{L}^{-1})$	—	50	—
emulgator/ ( $\text{mg}\cdot\text{L}^{-1}$ )	—	—	50
lactic acid/ ( $\text{g}\cdot\text{L}^{-1}$ )	22	—	6
ammonium sulfate/ ( $\text{g}\cdot\text{L}^{-1}$ )	—	6	—
surfactant/ ( $\text{mg}\cdot\text{L}^{-1}$ )	40	40	40

## 2.3 Characterization and testing

### 2.3.1 Surface morphology, composition and microstructure

The surface morphology and composition of single-layer coating and three-layer coating are characterized and analyzed by MERLIN Compact scanning electron microscope and X-max50 energy

dispersive spectrometer. The acceleration voltage of scanning electron microscope is 10 kV and the magnification is 6000 times. The energy spectrometer is set to surface scan mode, and the detection depth is 1  $\mu\text{m}$ . The image captured by scanning electron microscope is imported into Image J software, and the image characteristics are extracted. The holes on the surface of single-layer coating and three-layer coating are filled with red, and the ratio of the red area to total area of the image is defined as the porosity. The corrosion pits formed on the surface of single-layer coating and three-layer coating after corrosion are also filled with red, and the ratio of the red area to total image area is defined as the corrosion area ratio. In addition, the X'Pert PRO X-ray diffraction is used to characterize the microstructure of single-layer coating and three-layer coating. The scanning rate is  $4^\circ/\text{min}$ , from  $20^\circ$  to  $90^\circ$ .

### 2.3.2 Corrosion resistance testing

The 45# steel substrate, single-layer coating and three-layer coating samples are prepared as working electrodes suitable for electrochemical testing. Copper wire is welded on the back and the other areas are sealed with epoxy resin. Saturated calomel electrode is used as reference electrode and platinum plate is as auxiliary electrode. The polarization curves of samples immersed in 3.5% sodium chloride solution for different time are scanned at a constant rate of 1 mV/s. In addition, the protection efficiency of single-layer coating and three-layer coating on 45# steel is calculated according to the corrosion current density.

The 45# steel substrate, single-layer and three-layer coating samples are immersed in 3.5% sodium chloride solution to test the corrosion rate and observe the corrosion morphology to further evaluate their corrosion resistance. The experimental temperature is  $(25\pm 1)^\circ\text{C}$ , and the immersion time is 0~14 days. The corrosion products on the surface of the samples are removed and cleaned. And then, an electronic balance is used to weigh and record the quality of the samples before and after corrosion. The corrosion rate is calculated according to the following formula.

$$V_{corr} = \frac{(m_{before} - m_{after}) \cdot K}{S \cdot t \cdot \rho} \quad (1)$$

Where,  $V_{corr}$  is the corrosion rate, and unit is  $\text{g}/(\text{cm}^2 \cdot \text{a})$ .  $m_{before}$  and  $m_{after}$  are the mass of the sample before and after corrosion respectively, and the unit is g.  $K$  is a constant, which is usually as 87600;  $S$  is the surface area of the sample, the unit is  $\text{cm}^2$ ;  $t$  is the immersion time, the unit is h;  $\rho$  is the sample density, the unit is  $\text{g}/\text{cm}^3$ .

## 3. RESULTS AND DISCUSSION

### 3.1 Surface morphology

Figure 2 shows the surface morphology and porosity of 45# steel substrate, single layer coating and three-layer coating. By observing Figure 2(b) and Figure 2(c), it is found that the single-layer coating and three-layer coating completely cover the 45# steel substrate, and their surface are smooth

and uniform with granular morphology. The Ni-P coating with granular particles is also reported in some published papers [19-20]. However, there are more holes on the surface of single-layer coating, and fewer holes on the surface of three-layer coating. The surface compactness of three-layer coating is better than that of single-layer coating. This is because the bottom, intermediate and outer layer is different types of coatings, which are successively superimposed and deposited. As the cells are not neatly arranged on the surface of coating, the dislocation of three-layer coating is increased, thus improving the density of the coatings.

The porosity of three-layer coating is only 1.54%, which is significantly lower than that of single-layer coating 3.05%, indicating that the surface compactness of three-layer coating is better.

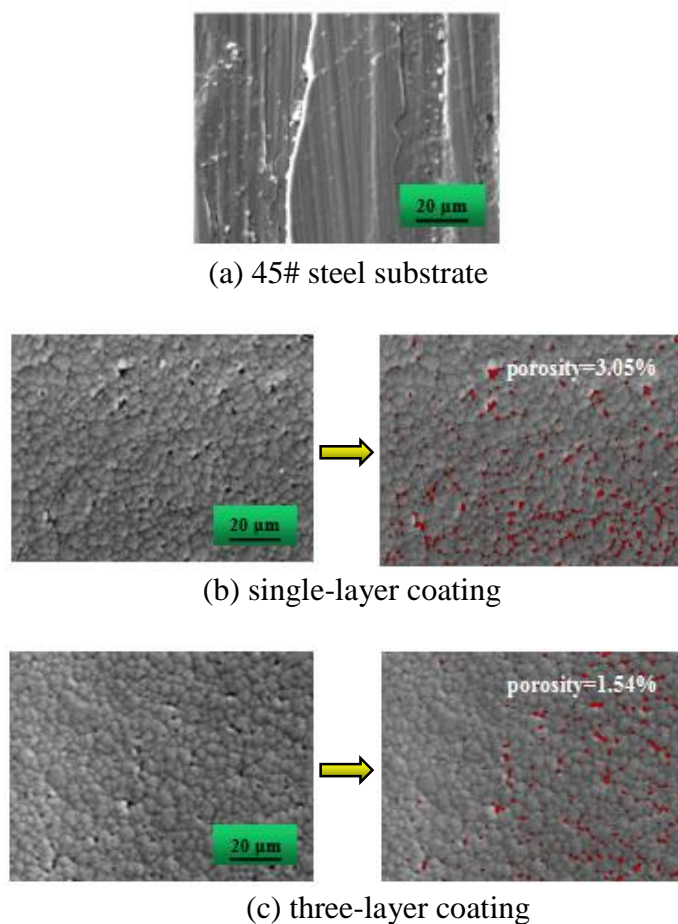


**Figure 2.** Surface morphology and porosity of 45# steel substrate, single-layer coating and three-layer coating. The acceleration voltage of scanning electron microscope is 10 kV and the magnification is 6000 times.

### 3.2 Microstructure and composition

Figure 3 shows the XRD patterns of 45# steel substrate, single-layer coating and three-layer coating. It can be seen from Figure 3(a) that the XRD pattern of 45# steel substrate shows multiple diffraction peaks, indicating that it has a crystalline structure. It can be seen from Figure 3(b) and Figure 3(c) that the XRD patterns of single-layer coating and three-layer coating are obviously

different from those of 45# steel substrate, which both show a broaden diffraction peak with high intensity corresponding to (111) crystal plane and several sharp diffraction peaks with low intensity corresponding to (220) crystal plane. This shows that the single-layer coating and three-layer coating have amorphous structures with a small amount of microcrystalline structures. The amorphous structure of Ni-P alloy coating has been reported in detail in some papers so far [21-23].

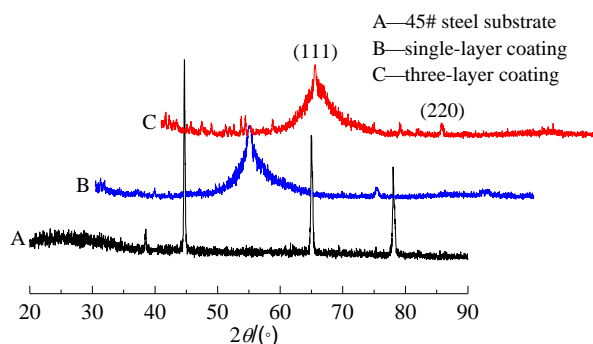


**Figure 3.** XRD patterns of 45# steel substrate, single-layer coating and three-layer coating. The scanning rate is 4°/min, from 20° to 90°.

Figure 4 shows EDS spectra of single-layer coating and three-layer coating. According to the analysis in Figure 4(a), the main composition of single-layer coating is Ni and P elements, of which the mass fraction of P element is 8.17%. According to the analysis in Figure 4(b), the main composition of three-layer coating is Ni, P and W elements, in which the mass fraction of P element is 12.48% and W element is 6.37%. According to the mass fraction of P element, the coating can be divided into low phosphorus coating (1%~4%), medium phosphorus coating (4%~10%) and high phosphorus coating (more than 10%). Therefore, it can be inferred that the single-layer coating is medium phosphorus coating, and the three-layer coating is high phosphorus coating. It is found that the content of phosphorus has a certain effect on the morphology, structure and corrosion resistance of alloy materials [24-27].

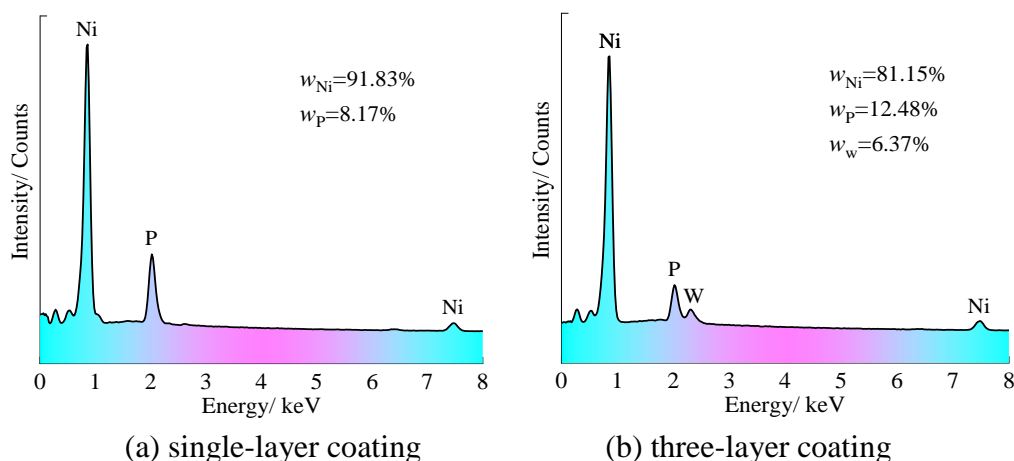


**Figure 4.** EDS spectra of single-layer and coating three-layer coating; The energy spectrometer is set to surface scan mode, and the detection depth is 1  $\mu\text{m}$ .

### 3.3 Corrosion resistance

Figure 5 shows the polarization curves of 45# steel substrate, single-layer coating and three-layer coating immersed in 3.5% sodium chloride solution for different time. Table 2 shows the fitting results of polarization curves. As can be seen from Figure 5, the corrosion potential of single-layer coating without immersion is about 70 mV higher than that of 45# steel substrate, and the corrosion current density is  $3.16 \times 10^{-6}$  A/cm<sup>2</sup>, which is about one order of magnitude lower than that of 45# steel substrate. Compare with 45# steel substrate, the corrosion potential of the three-layer coating moves about 113 mV, and the corrosion current density decreases by more than one order of magnitude (nearly two orders of magnitude). After immersion in 3.5% sodium chloride solution for 7 days, the corrosion potential of 45# steel substrate, single-layer coating and three-layer coating all shift negatively and the corrosion current density increase. The corrosion current density of 45# steel substrate increases to  $1.87 \times 10^{-4}$  A/cm<sup>2</sup> as the immersion time prolongs to 14 days. The corrosion current density of single-layer coating increases to  $1.12 \times 10^{-5}$  A/cm<sup>2</sup>, which also shows a trend of gradual increase, while the corrosion current density of three-layer coating increases very slowly.

Because the single-layer and three-layer coating completely cover the 45# steel substrate, and their surface are smooth and uniform, which can effectively prevent corrosive ions from contacting with 45# steel substrate, so as to improve the corrosion resistance. However, after immersion in 3.5% sodium chloride solution for a long time, the corrosion degree of chloride ions on the coating is gradually aggravated, which will destroy the surface structure of the coating and generate a layer of corrosion products covering the surface of single-layer and three-layer coating. Due to the potential difference between the bottom layer, intermediate layer and outer layer, the corrosion mechanism is different from that of single-layer coating, and the corrosion difficulty is increased. In addition, a relatively stable and dense corrosion products film is formed on the surface of three-layer coating, which effectively prevents further penetration of chloride ions, so that the corrosion current density of three-layer coating is maintained at a low level. Some researchers also investigate the effect of immersion time on the corrosion of metals [28-30]. It is found that at the initial stage of immersion, the corrosion current density of metal increases obviously. The increasing rate of corrosion current density of metal with good corrosion resistance decreases gradually with the extension of immersion time. It is because the early corrosion is mainly pitting corrosion. With the increase of immersion time, dense or loose corrosion products covering the metal surface delay the corrosion to a certain extent.

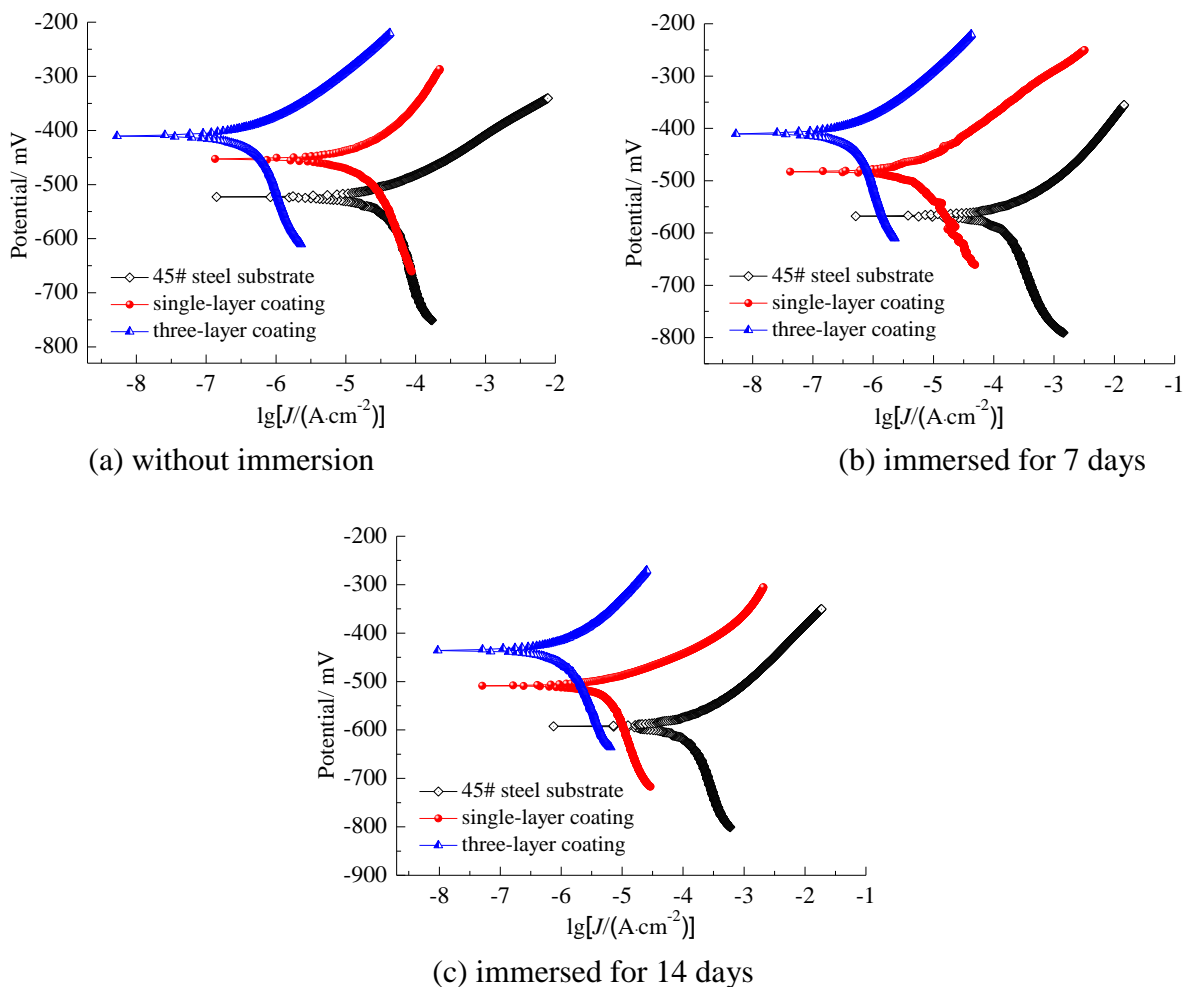


**Figure 5.** Polarization curves of 45# steel substrate, single-layer coating and three-layer coating immersed in 3.5% sodium chloride solution for different time; The different sample (1 cm×1 cm) is as the working electrode, saturated calomel electrode is as reference electrode and platinum plate is as auxiliary electrode. The scanning rate is 1 mV/s.

**Table 2.** Fitting results of polarization curves

Different samples	Corrosion potential/ mV			Corrosion current density/ (A·cm <sup>-2</sup> )		
	Without immersion	Immersed for 7 days	Immersed for 14 days	Without immersion	Immersed for 7 days	Immersed for 14 days
45# steel substrate	-523	-567	-592	4.05×10 <sup>-5</sup>	9.42×10 <sup>-5</sup>	1.87×10 <sup>-4</sup>
single-layer coating	-453	-482	-508	3.16×10 <sup>-6</sup>	5.40×10 <sup>-6</sup>	1.12×10 <sup>-5</sup>
three-layer coating	-410	-425	-436	7.24×10 <sup>-7</sup>	9.78×10 <sup>-7</sup>	1.04×10 <sup>-6</sup>

According to the corrosion current density, the protection efficiency of single-layer coating and three-layer coating on 45# steel substrate immersed in 3.5% sodium chloride solution for different time

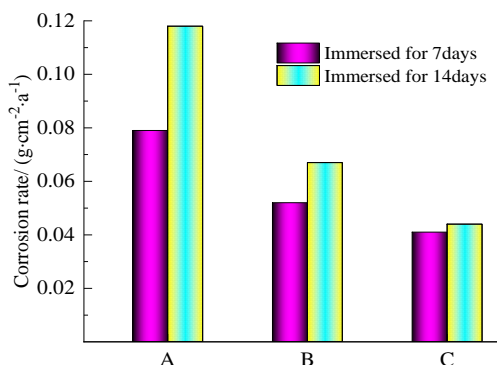
is calculated, as shown in Table 3. It can be seen from Table 3, with the extension of immersion time, the protection efficiency of single-layer coating on 45# steel substrate tends to increase firstly and then decrease, while that of three-layer coating on 45# steel substrate tends to increase gradually.

Generally speaking, higher protection efficiency indicates that the coating can effectively prevent corrosive ions from contacting the substrate, thus providing better protection [31-32]. Combined with the analysis of corrosion current density and the protection efficiency of 45# steel substrate, the corrosion resistance of three-layer coating is better than that of single-layer coating. The reason is that three-layer coating has low porosity and good surface compactness, which enhance resistance to corrosive ions showing higher electrochemical corrosion resistance. According to the corrosion current density, the protection efficiency of single-layer coating and three-layer coating on 45# steel substrate is 92.3% and 98.2%, respectively. Based on the analysis of corrosion potential, corrosion current density, polarization resistance and protection efficiency, the corrosion resistance of three-layer coating is better than that of single-layer coating.

**Table 3.** Protection efficiency of single-layer coating and three-layer coating on 45# steel substrate immersed in 3.5% sodium chloride solution for different time

Different samples	Protection efficiency / %		
	Without immersion	Immersed for 7 days	Immersed for 14 days
single-layer coating	92.2	94.3	94.0
three-layer coating	98.2	98.9	99.4

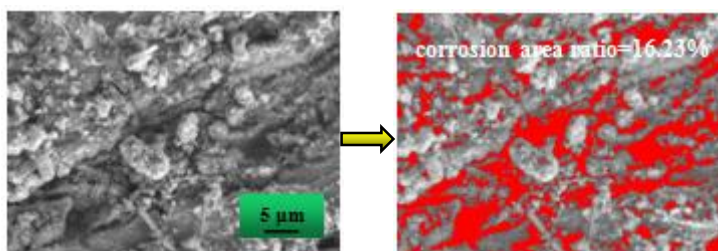
Figure 6 shows the corrosion rate of 45# steel substrate, single-layer coating and three-layer coating immersed in 3.5% sodium chloride solution for different time. The corrosion rate of 45# steel substrate is the highest, reaching 0.118 g/(cm<sup>2</sup>·a). The corrosion rate of single-layer coating is 0.067 g/(cm<sup>2</sup>·a), which is 43.2% lower than that of 45# steel substrate. The lowest corrosion rate of three-layer coating is only 0.044 g/(cm<sup>2</sup>·a), which is 62.7% and 34.3% lower than that of 45# steel substrate and single-layer coating, respectively. Generally speaking, the lower the corrosion rate, the slower the corrosion of the materials in corrosive medium, and its corrosion resistance is excellent. The variation of corrosion rate further indicates that three-layer coating has higher electrochemical corrosion resistance. Due to its low porosity and good surface compactness, it can effectively prevent the contact between chloride ions and 45# steel substrate, thus reducing the corrosion degree and showing better corrosion resistance.



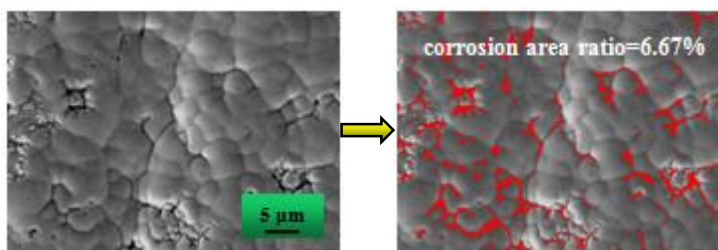
**Figure 6.** Corrosion rate of 45# steel substrate, single-layer coating and three-layer coating immersed in 3.5% sodium chloride solution for different time: A-45# steel substrate; B-single-layer coating; C-three-layer coating

Figure 7 shows the corrosion morphology and corrosion area ratio of 45# steel substrate, single-layer coating and three-layer coating immersed in 3.5% sodium chloride solution for 14 days. It can be seen from Figure 7(a) that 45# steel substrate corrodes very seriously with a loose porous layer and a deep crevice formed on its surface. It can be seen from Figure 7(b) that after immersing in 3.5% sodium chloride solution for 14 days, some penetrating holes are formed on the surface of single-layer coating. The local holes are larger, and the unit cell is also damaged. It can be seen from Figure 7(c) that after immersing in 3.5% sodium chloride solution for 14 days, a small number of holes are formed on the surface of three-layer coating, and the unit cell is basically not damaged.

The corrosion area ratio of 45# steel substrate, single-layer coating and three-layer coating is 16.23%, 6.67% and 2.86%, respectively. Generally speaking, the higher the area ratio, the more holes and gaps formed on the surface after corrosion. The corrosion area ratio of three-layer coating is the lowest, and its corrosion degree is significantly reduced compared with that of single-layer coating, which further indicates that the corrosion resistance of three-layer coating is better than that of single-layer coating.



(a) 45# steel substrate



(b) single-layer coating

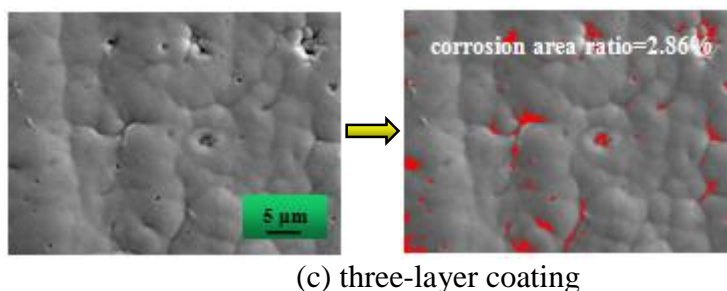


**Figure 7.** Corrosion morphology and corrosion area ratio of 45# steel substrate, single-layer coating and three-layer coating immersed in 3.5% sodium chloride solution for 14 days

#### 4. CONCLUSIONS

Ni-P/Ni-W-P/Ni-P three-layer coating with amorphous structure and excellent corrosion resistance was prepared on the surface of 45# steel substrate by chemical deposition method. The main composition of three-layer coating is Ni, P and W elements. The prepared three-layer coating belonged to the coating with high phosphorus content, while Ni-P single-layer coating belonged to the coating with medium phosphorus content. Compared with single-layer coating, three-layer coating has better surface compactness, lower corrosion current density, smaller corrosion rate and higher electrochemical corrosion resistance, which can provide better protection for 45# steel substrate.

#### ACKNOWLEDGEMENT

The study was supported by Yulin Science and Technology Department, China (Grant No. CXY-2020-006-03), (Grant No. CXY-2020-006-06), (Grant No. CXY-2020-005-04) and (Grant No. CXY-2021-101-02); Yulin Gaoxing Science and Technology Department, China (Grant No. CXY-2021-35) and (Grant. YLU-DNL Fund 2021004), The Key Research and Development Program of Shaanxi Provincial Science and Technology Department (2022SF-456), and Key Laboratory Project of low metamorphic coal in Shaanxi Province (20JS162).

#### References

1. E. M. Fayyad, M. K. Hassan, K. Rasool, K. A. Mahmoud, A. M. A. Mohamed, G. Jarjoura, Z. Farhat and A. M. Abdullah, *Surf. Coat. Technol.*, 369 (2019) 323.
2. A. Lelevic and F. C. Walsh, *Surf. Coat. Technol.*, 369 (2019) 198.
3. V. S. Sumi, M. A. Sha, S. R. Arunima and S. M. A. Shibli, *Electrochim. Acta*, 303 (2019) 67.
4. Y. H. Hu, Y. D. Yu, H. L. Ge, G. Y. Wei and L. Jiang, *Int. J. Electrochem. Sci.*, 14 (2019) 1649.
5. Q. Y. Wang, S. Liu, Y. R. Tang, R. Pei, Y. C. Xi and D. X. Zhang, *Int. J. Electrochem. Sci.*, 14 (2019) 3740.
6. E. M. Fayyad, P. A. Rasheed, N. Al-Qahtani, A. M. Abdullah, F. Hamdy, M. A. Sharaf, M. K. Hassan, K. A. Mahmoud, A. M. Mohamed, G. Jarjoura and Z. Farhat, *Arabian J. Chem.*, 14 (2021) 103445.
7. D. Figuet, A. Billard, C. Savall, J. Creus, S. Cohendoz and J. L. Grosseau-Poussard, *Mater. Chem. Phys.*, 276 (2022) 125332.
8. R. Q. Li, Q. J. Dong, J. Xia, C. H. Luo, L. Q. Sheng, F. Cheng and J. Liang, *Surf. Coat. Technol.*,

- 366 (2019) 138.
9. V. Vitry, J. Hastir, A. Megret, S. Yazdani, M. Yunacti and L. Bonin, *Surf. Coat. Technol.*, 429 (2022) 127937.
  10. A. Solimani, T. M. Meibner, C. Oskay and M. C. Galetz, *Sol. Energy Mater. Sol. Cells*, 231 (2021) 111312.
  11. J. T. Wang, X. L. Bai, X. H. Shen, X. F. Liu and B. L. Wang, *J. Manuf. Processes*, 74 (2022) 296.
  12. P. Kanagavalli, C. Andrew, M. Veerapandian and M. Jayakumar, *TrAC, Trends Anal. Chem.*, 143 (2021) 116413.
  13. I. Sultana, A. Masood, Z. Shoukat, A. Arshad, S. O. Hussain, G. M. Mustafa, S. Atiq and A. Razaq, *Ceram. Int.*, 45 (2019) 11141.
  14. V. Torabinejad, M. Aliofkhaezrai, A. S. Rouhaghdam and M. H. Allahyarzadeh, *Tribol. Int.*, 106 (2017) 34.
  15. V. Torabinejad, A. S. Rouhaghdam, M. Aliofkhaezrai and M. H. Allahyarzadeh, *J. Alloys Compd.*, 657 (2016) 526.
  16. B. Bahadormanesh and M. Ghorbani, *Appl. Surf. Sci.*, 442 (2018) 275.
  17. A. Dolati and S. S. Mahshid, *Mater. Chem. Phys.*, 108 (2008) 391.
  18. B. Tunaboylu, *Mater. Lett.*, 70 (2012) 51.
  19. S. Alleg, A. Boussaha, W. Tebib, M. Zergoug and J. J. Sunol, *J. Supercond. Novel Magn.*, 29 (2016) 1001.
  20. C. Benyekken, A. Benhaya, F. Djeflal and M. Chahdi, *Trans. Electr. Electron. Mater.*, 23 (2022) 52.
  21. S. Samanta, K. Mondal, M. Dutta and S. B. Singh, *Surf. Coat. Technol.*, 409 (2021) 126928.
  22. G. M. Song, Y. Wu, Q. Xu and G. Liu, *J. Power Sources*, 195 (2010) 3913.
  23. J. T. W. Jappes, N. C. Brintha and M. A. Khan, *Mater. Today: Proc.*, 46 (2021) 7230.
  24. J. C. Han, A. P. Liu, J. Q. Zhu, M. L. Tan and H. P. Wu, *Appl. Phys. A*, 88 (2007) 341.
  25. J. Lou, K. Yu, G. Wei, C. Xin, Y. Qin, L. Jiang, H. Ge and H. Dettinger, *Surf. Eng.*, 29 (2013) 637.
  26. N. Kovalska, W. E. G. Hansal, N. Tsyntaru, H. Cesiulis, A. Gebert and W. Kautek, *Trans. Inst. Met. Finish.*, 97 (2019) 89.
  27. W. T. Tsai and S. T. Chung, *J. Supercrit. Fluids*, 95 (2015) 292.
  28. H. M. Zhang, L. Yan, Y. Y. Zhu, F. F. Ai, H. N. Li, Y. Li and Z. Y. Jiang, *Metals*, 11 (2021) 1317.
  29. V. Asadi, I. Danaee and H. Eskandari, *J. Mater. Eng.*, 18 (2015) 706.
  30. L. H. Jiang, W. W. Dai, Z. Wei, Y. F. Huang, F. X. Wang and S. Hong, *Surf. Topogr. Metrol. Prop.*, 10 (2022) 1.
  31. R. Rajkumar and C. Vedhi, *Vacuum*, 161 (2019) 1.
  32. B. V. A. Rao and M. N. Reddy, *Arabian J. Chem.*, 10 (2017) 3270.